Research Article

Engineering: Open Access

Control System for Improved Performance in PLUG-in Hybrid Electric Vehicles (PHEV)

C. Armenta-Déu*

Facultad de Ciencias Físicas. Universidad Complutense de Madrid, Spain

***Corresponding Author**
C. Armenta-Déu, Facultad de Ciencias Físicas. Universidad Complutense de Madrid, Spain.

Submitted: 2025, Nov 03; **Accepted**: 2025, Nov 28; **Published**: 2025, Dec 02

Citation: Armenta-Déu, C. (2025). Control System for Improved Performance in PLUG-in Hybrid Electric Vehicles (PHEV). *Eng OA, 3*(12), 01-14.

Abstract

This paper aims at designing a control system that regulates the electric motor in Plug-in Hybrid Electric Vehicles (PHEV) to optimize the vehicle performance, extending the driving range and minimizing the energy consumption. The method bases on controlling the electric motor engagement, to maximize the delivered energy from the battery, maintaining driving conditions within specific limits, and combining combustion engine and electric motor to help the vehicle in saving energy while running. The proposed protocol consists of a regulation of vehicle speed and acceleration depending on driving conditions and road orography. The protocol specially applies for urban routes, where the appropriate use of the electric motor optimizes the battery performance, the fuel consumption, and vehicle driving range. The carried out simulation shows that the driving range extension may reach near 172% of current value under standard driving operations for the worst driving conditions (aggressive mode). The driving range extension results from adequate management of the dual power source, limiting electric motor use during daily journeys to an optimal value that depends on the driving mode and vehicle speed range. The operational range of the electric motor daily fractional time varies from 66.9% to 92.4% in diesel PHEVs, and from 47.7% to 89% in gasoline PHEVs. The dual power source management requires a control system to regulate the combustion engine and electric motor, following a protocol to maximize vehicle performance, minimizing energy consumption, and reducing greenhouse gas emissions.

1. Introduction

The continuous growth of GHG emissions from vehicles generates a progressive increase in pollution levels in urban areas, especially in congested cities, reducing air quality and causing health problems. Local, regional, national, and supranational authorities promote a transition from internal combustion engine (ICE) cars to electric vehicles (EVs) [1-4]. A rapid transition from ICE cars to EVs results in technical, social, and economic problems; therefore, the modern trend is a gradual implementation of electric vehicles through a combination of hybrid (HEV), plug-in hybrid (PHEV), and electric vehicle (BEV) [5-9].

Today, there are significant differences in electric vehicles' sales in the car sales market due to vehicle costs and citizens' purchasing power [10-14]. To minimize the impact of purchasing electric vehicles on car buyers, authorities enact incentive policies through purchase subsidies, showing variable results [15-22]. In some countries, more than 50% of local sales are electric vehicles, while in others the percentage is 10% [23-26]. Battery electric vehicles (BEVs) represent a challenge to modern society due to numerous associated problems and driver reluctance stemming from their shorter range and dependence on the electrical grid for charging. This situation is a critical point for the acceptance of electric vehicles among drivers, since a depleted battery means the car must stop immediately, with no possibility of refueling at a gas station with a small fuel tank to resume current driving [12, 27-33].

To avoid the problem of battery depletion and dependence on refueling at a gas station, the plug-in hybrid electric vehicle (PHEV) emerges as the optimal solution. It can operate independently using either the internal combustion engine or the electric motor; if the battery runs out, the internal combustion engine powers the car until it reaches the nearest charging point or the driver's home. This configuration is advantageous for PHEVs compared to battery electric vehicles without an internal combustion engine option, or HEVs that also have a dual power source (internal combustion engine and battery) but require the internal combustion engine to be running to charge the battery, thus reducing the independence of the dual power source [34-35].

Nevertheless, driving plug-in hybrid electric vehicles (PHEVs) is

controversial, as it involves analyzing the fuel consumption and environmental impact. In fact, if an internal combustion engine (ICE) powers the plug-in hybrid electric vehicle, fuel consumption increases due to the battery weight. Statistical data shows that, in most cases, drivers use the PHEV with the ICE engine, dispensing with the battery, either to conserve extra energy for emergencies or simply because it has run down due to lack of regular charging, for convenience, or out of negligence [36]. The internal combustion engine in plug-in hybrid vehicles not only increases overall fuel consumption but also greenhouse gas emissions, which in many cases are even higher than those of a conventional fossil-fuel car [37]. This situation has raised concerns among authorities regarding the benefits of plug-in hybrid vehicles and, consequently, led to the decision to limit their promotion [38].

Today, there are different strategies to control the PHEV performance. Amonsg them, we can mention energy management algorithms , Markov chains, PHEV variable controllers, Powertrain Systems Analysis Toolkit (PSAT), global optimization algorithm, based on the Bellman principle, Equivalent Consumption Minimization Strategy (ECMS), and Machine Learning [39-46]. In this article, we develop a new protocol for the operation of plug-in hybrid electric vehicles to improve performance through optimal battery energy management, thereby reducing fuel consumption and greenhouse gas emissions. This protocol represents a significant advancement in the current state of the art for driving plug-in hybrid vehicles and ensures efficient use of battery energy.

2. Situation Background

Plug-in hybrid electric vehicles use a dual power source for propulsion: a fossil fuel internal combustion engine, either diesel or gasoline, and an electric motor powered by a battery. Both power sources operate independently, according to a set protocol that selects which one activates at any given time. The electric motor in a plug-in hybrid starts automatically when you begin driving if the battery has sufficient charge. The car prioritizes the electric motor for propulsion, especially in the city and at low speeds, until the battery depletes or the vehicle requires more power for strong acceleration or highway driving. In urban areas, where sudden acceleration or high speeds are infrequent, the PHEV operates on electric power as long as the battery is charged. However, in many cases, the driver forgets to charge the battery or travels distances exceeding the available electric range. In this situation, the ICE engages and the PHEV operates as a conventional car with a combustion engine, with the significant difference of a higher mass due to the battery's weight. The greater mass of the vehicle generates an increase in fuel consumption and gas emissions, exceeding the values of an identical vehicle with propulsion solely by a combustion engine.

3. Theoretical Background

The driving force, F_{dr}, which propels the vehicle, depends on the dynamic conditions expressed in the following equation:

$$F_{dr} = ma + \kappa v + mg(\mu + \sin\alpha) \quad (1)$$

m is the vehicle global mass, κ and μ are the drag and rolling coefficients, a and v are the vehicle acceleration and speed, and α is the road slope.

The energy consumption associated with the driving force is:

$$\xi_{dr} = \left[mav + \kappa v^2 + mg(\mu + \sin\alpha)v \right] t_{dr} \quad (2)$$

t_{dr} is the driving time.

Because a vehicle never runs at constant speed during an entire daily journey, it is necessary to divide the daily journey into segments of unchanged speed; therefore, Equation 2 transforms into:

$$\xi_{dr} = \sum_{i=1}^{n} \left[ma_i v_i + \kappa v_i^2 + mg(\mu + \sin\alpha_i)v_i \right] t_{dr,i} \quad (3)$$

Considering the pavement type is regular. The subscript i represents the segment number, with n being the total number of segments.

The energy for driving shown in Equation 3 proceeds from the ICE or the electric motor. For equal driving conditions, we can compare the fuel and battery consumption in a complete daily journey; in such a situation, we have for a combustion engine:

$$\xi_{dr} = \frac{Q_f \rho_f}{\eta_f} \sum_{i=1}^{n} C_{f,i} d_i = \frac{Q_f \rho_f}{\eta_f} V_f^{day} = K_f V_f^{day} \quad (4)$$

Q is the combustion heat power, C is the consumption rate, ρ is the density, η is the engine efficiency, and d is the driving distance. The subscript f accounts for the fossil fuel, diesel and gasoline. V_f^{day} represents the volume of fuel consumed in a daily journey.

If the battery supplies the energy:

$$\xi_{dr} = V_{bat}^{ave} I t_{dr} \quad (5)$$

V_{bat}^{ave} is the battery average voltage for the discharge process, and I is the discharge current.

Because the energy to propel the PHEV during the daily journey is a combination of the dual power source, ICE and battery, we can establish:

$$\xi_{dr} = f_{ICE} K_f V_f^{day} + f_{EM} V_{bat}^{ave} I t_{dr} \quad (6)$$

The coefficients f_{ICE} and f_{EM} represent the ICE and electric motor operational fraction time of a daily journey; therefore, the following condition fulfils $f_{ICE}+f_{EM}=1$ (7).

The driving optimum performance corresponds to the minimum of energy consumption. Applying this condition to Equation 6, we obtain:

$$\frac{d\xi_{dr}}{dt} = \frac{d}{dt}\left(f_{ICE} K_f V_f^{day} + f_{EM} V_{bat}^{ave} I t_{dr} \right) = 0 \quad (8)$$

Operating in Equation 8:

$$f_{ICE} K_f \frac{dV_f^{day}}{dt} + f_{ICE} V_f^{day} \frac{dK_f}{dt} + K_f V_f^{day} \frac{df_{ICE}}{dt} + \\ + f_{EM} V_{bat}^{ave} I \frac{dt_{dr}}{dt} + f_{EM} V_{bat}^{ave} t_{dr} \frac{dI}{dt} + f_{EM} I t_{dr} \frac{dV_{bat}^{ave}}{dt} + V_{bat}^{ave} I t_{dr} \frac{df_{EM}}{dt} = 0 \quad (9)$$

Retrieving K_f from Equation 4, applying Equation 7, considering

the battery average voltage constant, and expressing the daily fuel consumption, V_f^{day} as:

$$V_f^{day} = \frac{(\xi_{dr} - \xi_{EM})\eta_f}{Q_f \rho_f} \tag{10}$$

With:

$$\xi_{EM} = f_{EM}\xi_{dr}\,;\, \xi_{ICE} = f_{ICE}\xi_{dr} \tag{11}$$

Equation 9 transforms into:

$$\left(\frac{\left(1+f_{EM}^2-2f_{EM}\right)\xi_{dr} - Q_f\rho_f(1-f_{EM})V_f^{day}}{\eta_f}\right)\frac{d\eta_f}{dt} + \\ + \left(\frac{Q_f\rho_f V_f^{day}}{\eta_f} + V_{bat}^{ave} I t_{dr} + f_{EM}\xi_{dr} - \xi_{dr}\right)\frac{df_{EM}}{dt} + f_{EM}V_{bat}^{ave}\left(I + t_{dr}\frac{dI}{dt}\right) = 0 \tag{12}$$

For a fixed f_{EM} value, combining Equations 5, 10 and 12, we have:

$$(1-f_{EM})^2\xi_{dr}\left(\frac{1-\eta_f}{\eta_f}\right)\frac{d\eta_f}{dt} + \frac{f_{EM}\xi_{dr}}{t_{dr}} + f_{EM}V_{bat}^{ave}t_{dr}\frac{dI}{dt} = 0 \tag{13}$$

Analyzing equation 13, we observe three distinct terms. The first, on the left, shows a dependence of the internal combustion engine and the electric motor through the internal combustion engine efficiency (η_f) and the electric motor operating time (*fEM*). The second depends solely on the electric motor operating time. The third depends on the electric motor operating time and the battery performance as a function of the evolution of the discharge current (*dI/dt*).

We can consider the efficiency of an internal combustion engine (ICE) as a constant value in general terms for daily driving; however, it varies with driving conditions, acceleration, constant speed, and deceleration. Therefore, we assume that the term η_f does not change, but its variation over time does. A similar situation occurs with the discharge current, since it depends on the power demand, which in turn depends on driving conditions.

The preliminary analysis requires segmenting the daily commute into three groups: acceleration, deceleration, and constant speed. It is evident that acceleration is not uniform across all segments; therefore, we apply three acceleration values: high, medium, and low (a_s, a_m, and a_c), corresponding to the sport, moderate (normal), and conservative driving modes, respectively. For deceleration, we use a single value, ad, representing the braking mode. In constant speed mode, the values differ between segments, as they do in acceleration mode; however, we apply the same criteria, using three distinct values (v_s, v_m, and v_c) for the sport, moderate (normal), and conservative modes, respectively.

On the other hand, the performance of a combustion engine inversely depends on acceleration, according to a second-degree relation of the following type:

$$\eta_f = C_2 a^2 - C_1 a + C_o \tag{14}$$

Table 1 lists the coefficients values for diesel and gasoline engines.

Engine	C_2	C_1	C_o	R^2
Diesel	1.678	10.247	45.415	0.9983
Gasoline	0.5217	3.2072	29.886	0.9989

Table 1: Correlation Coefficients for the Diesel and Gasoline Engine Efficiency as a Function of the Acceleration

Applying the Dynamics laws, the acceleration at any segment is given by:

$$a = \frac{v_f - v_i}{t} = \frac{\Delta v}{t} \tag{15}$$

If the initial and final vehicle speed, v_f and v_i, are fixed, the derivative of engine efficiency regarding time is:

$$\frac{d\eta_f}{dt} = 2C_2\frac{(\Delta v)^2}{t^3} - C_1\frac{\Delta v}{t^2} \tag{16}$$

Because we have three acceleration segments:

$$\frac{d\eta_f}{dt} = 2C_2\frac{(\Delta v_s)^2 + (\Delta v_m)^2 + (\Delta v_c)^2}{t^3} - C_1\frac{\Delta v_s + \Delta v_m + \Delta v_c}{t^2} \tag{17}$$

Using Equation 5, the derivative of the discharge current is:

$$\frac{dI}{dt} = \frac{1}{V_{bar}^{ave}}\left[F_{dr}a + v\left(m\frac{da}{dt} + k\frac{d(v^2)}{dt} + mg\frac{d}{dt}(\mu + \sin\alpha)\right)\right] \tag{18}$$

Since the acceleration remains constant in the analyzed segment, and *m*, μ, and α, are constant too, Equation 18 transforms into:

$$\frac{dI}{dt} = \frac{F_{dr}a + 2kv^2a}{V_{bar}^{ave}} \tag{19}$$

Considering the acceleration term as the prevalent in the driving force (see Table 2):

$$\frac{dI}{dt} = \frac{ma^2 + 2kv^2a}{V_{bar}^{ave}} \tag{20}$$

Where *v* represents the average vehicle speed in the segment for a specific acceleration.

	Force term			
Driving mode	Accel.	Drag	Rolling	Ratio
Sport	8750	355	368	0.92
Moderate	5625	171	368	0.91
Conservative	3750	61	368	0.90

Table 2: Ratio Between Acceleration Term and Overall Driving Force

Data in Table 2 correspond to a standard PHEV running in urban zone at different driving modes.

Replacing Equations 17 and 20 in Equation 13:

$$(1-f_{EM})^2\xi_{dr}\left(\frac{1-\eta_f}{\eta_f}\right)\left[2C_2\frac{(\Delta v_s)^2 + (\Delta v_m)^2 + (\Delta v_c)^2}{t^3} - C_1\frac{\Delta v_s + \Delta v_m + \Delta v_c}{t^2}\right] - \\ - \frac{f_{EM}\xi_{dr}}{t_{dr}} - f_{EM}V_{bat}^{ave}t_{dr}\left(\frac{ma^2 + 2kv^2a}{V_{bar}^{ave}}\right) = 0 \tag{21}$$

Equation 21 represents the condition for optimum performance of a PHEV operating with dual power mode, combustion engine and electric motor.

Following to this theoretical analysis, we develop a simulation study to establish the operational conditions to optimize the driving conditions in PHEVs.

4. Application Environment

Given the numerous plug-in hybrid electric vehicle (PHEV) models with varying masses, aerodynamic coefficients, and battery capacities, we selected three models representing high, medium, and low masses. Vehicle mass is considered a critical parameter in our study due to its significant influence on power demand and energy consumption; therefore, the three selected PHEVs correspond to heavy, medium-light, and light vehicle categories in the plug-in hybrid electric vehicle market.

The selected models are the Volvo XC90 for the high segment, the Ford Kuga for the intermediate, and the Toyota Prius for the low one. Table 3 shows the parameter values used in the simulation.

Model	Mass (kg)	Battery energy capacity (kWh)	Battery voltage (V)	Aerodynamic coefficient	Combustion engine efficiency (%)
Volvo XC90	2300	18.8	360	0.33	30-45 (D) 25-30 (G)
Ford Kuga	1860	14.4	360	0.27	
Toyota Prius	1600	8.8	250	0.24	

Table 3: Parameter Values Used in the Simulation for Three Types of PHEV

We observed a difference in battery energy capacity among the selected models, with the value increasing from the lower to the higher categories. However, due to the mass difference, the electric range is similar for all three models; around 70 km. We analyzed the relationship between vehicle mass and battery energy capacity to determine the suitability of these models regarding their electric range. Relating battery energy capacity and vehicle mass, we obtain a close relation for all the selected vehicles (see Table 4); therefore, we consider the selection appropriate for our study.

Model	Electric mode driving range (km)	Energy/mass coeff. ($\xi_{bat}/m^{1/2}$)
Volvo XC90 Recharge	71	0.0036
Ford Kuga	67	0.0042
Toyota Prius	71	0.0034

Table 4: Electric Mmode Driving Range and Energy/Mass Ratio for the sSelected PHEVs

The energy-to-mass coefficient is consistent across all cases, highlighting the appropriateness of the chosen vehicles for the simulation. We use this coefficient due to the non-linear relationship between battery energy and vehicle mass.

5. Simulation

The simulation study involves determining the variable parameter values needed to satisfy the condition outlined in Equation 21. This optimization focuses on improving the driving conditions for plug-in hybrid electric vehicles (PHEVs) that operate with an independent dual-energy powertrain comprising an internal combustion engine and an electric motor. The simulation runs for different driving modes—sport, moderate, and conservative—under urban conditions. Therefore, we use three different values for the acceleration and for the vehicle speed range. Table 5 lists the associated values for the three driving modes.

		Vehicle speed range (km/h)		
Driving mode	Acceleration (m/s^2)	Low	Medium	High
Sport	3.50	60-85	45-80	30-80
Moderate	2.25	50-70	40-70	35-70
Conservative	1.25	40-60	35-60	30-60

Table 5: Acceleration and Vehicle Speed Range for Standard Driving Modes in Urban Areas

We establish a speed range for each driving mode to accommodate the simulation to current driving conditions, in close agreement with drivers' attitudes and traffic conditions. Therefore, we consider for the simulation every driving mode with its characteristic acceleration and the three-vehicle speed ranges.

Tables 6 and 7 show the simulation results. The simulated EM energy use corresponds to the daily energy consumed by the PHEV in electric mode, considering the optimum fractional time for electric mode operation that fulfils Equation 21 condition. The simulated driving range in electric mode (EM-DR) is the available number of days the PHEV may run on electric mode if operating at optimum electric mode fractional time. The WLTP EM-DR is the PHEV standard driving range in electric mode according to the WLTP protocol. The estimated EM-DR datum corresponds to the corrected WLTP EM-DR value due to real driving conditions. Finally, the EM-DR ratio represents the PHEV driving range improvement for electric mode operation if applying the optimal fraction value.

Engine type Gasoline			Category High segment		PHEV model Volvo XC90		
Acc. (m/s^2)	Vehicle Speed range	f_{EM}	Simul. EM energy use (kWh)	Simul. EM-DR (days)	WLTP EM-DR (days)	Estimated EM-DR (days)	EM-DR ratio
3.5	Low	0.5326	4.330	4.342	2.219	2.313	1.877
	Medium	0.6482	5.270	3.568			1.543
	High	0.7444	6.052	3.107			1.343
2.25	Low	0.6553	5.327	3.529			1.526
	Medium	0.7499	6.096	3.084			1.334
	High	0.8230	6.691	2.810			1.215
1.25	Low	0.7723	6.278	2.994			1.295
	Medium	0.8406	6.834	2.751			1.190
	High	0.8901	7.236	2.598			1.123
Engine type Gasoline			Category Intermediate segment		PHEV model Ford Kuga		
Acc. (m/s^2)	Vehicle Speed range	f_{EM}	Simul. EM energy use (kWh)	Simul. EM-DR (days)	WLTP EM-DR (days)	Estimated EM-DR (days)	EM-DR ratio
3.5	Low	0.5270	3.420	4.210	2.094	2.219	1.898
	Medium	0.6441	4.180	3.445			1.552
	High	0.7416	4.813	2.992			1.349
2.25	Low	0.6492	4.213	3.418			1.540
	Medium	0.7458	4.840	2.975			1.341
	High	0.8204	5.325	2.704			1.219
1.25	Low	0.7659	4.970	2.897			1.306
	Medium	0.8367	5.430	2.652			1.195
	High	0.8878	5.762	2.499			1.126
Engine type Gasoline			Category Low segment		PHEV model Toyota Prius		
Acc. (m/s^2)	Vehicle Speed range	f_{EM}	Simul. EM energy use (kWh)	Simul. EM-DR (days)	WLTP EM-DR (days)	Estimated EM-DR (days)	EM-DR ratio
3.5	Low	0.4769	2.004	4.391	2.219	2.094	2.097
	Medium	0.6011	2.526	3.483			1.664
	High	0.7075	2.974	2.959			1.413
2.25	Low	0.6047	2.542	3.462			1.654
	Medium	0.7111	2.989	2.944			1.406
	High	0.7947	3.340	2.635			1.258
1.25	Low	0.7311	3.073	2.864			1.368
	Medium	0.8118	3.412	2.579			1.232
	High	0.8703	3.658	2.406			1.149

Table 6: Simulation Results for the Gasoline Gngine PHEV

Engine type Diesel			Category High segment		PHEV model Volvo XC90		
Acc. (m/s^2)	Vehicle Speed range	f_{EM}	Simul. EM energy use (kWh)	Simul. EM-DR (days)	WLTP EM-DR (days)	Estimated EM-DR (days)	EM-DR ratio
3.5	Low	0.6691	5.439	3.456	2.219	2.313	1.495
	Medium	0.7594	6.174	3.045			1.317
	High	0.8295	6.743	2.788			1.206
2.25	Low	0.7639	6.211	3.027			1.309
	Medium	0.8328	6.770	2.777			1.201
	High	0.8837	7.184	2.617			1.132
1.25	Low	0.8384	6.816	2.758			1.193
	Medium	0.8884	7.222	2.603			1.126
	High	0.9237	7.510	2.503			1.083

Engine type Diesel			Category Imtermediate segment		PHEV model Ford Kuga		
Acc. (m/s^2)	Vehicle Speed range	f_{EM}	Simul. EM energy use (kWh)	Simul. EM-DR (days)	WLTP EM-DR (days)	Estimated EM-DR (days)	EM-DR ratio
3.5	Low	0.6645	4.313	3.339	2.094	2.313	1.505
	Medium	0.7563	4.909	2.934			1.322
	High	0.8275	5.370	2.681			1.209
2.25	Low	0.7593	4.928	2.922			1.317
	Medium	0.8299	5.386	2.674			1.205
	High	0.8819	5.723	2.516			1.134
1.25	Low	0.8336	5.410	2.662			1.200
	Medium	0.8856	5.747	2.506			1.129
	High	0.9221	5.984	2.406			1.085

Engine type Diesel			Category Low segment		PHEV model Toyota Prius		
Acc. (m/s^2)	Vehicle Speed range	f_{EM}	Simul. EM energy use (kWh)	Simul. EM-DR (days)	WLTP EM-DR (days)	Estimated EM-DR (days)	EM-DR ratio
3.5	Low	0.6224	2.616	3.364	2.219	2.313	1.607
	Medium	0.7235	3.041	2.894			1.382
	High	0.8031	3.375	2.607			1.245
2.25	Low	0.7254	3.049	2.886			1.379
	Medium	0.8050	3.383	2.601			1.242
	High	0.8642	3.632	2.423			1.157
1.25	Low	0.8075	3.394	2.593			1.238
	Medium	0.8674	3.646	2.414			1.153
	High	0.9097	3.823	2.302			1.099

Table 7: Simulation Results for the Diesel Engine PHEV

6. Simulation Results Analysis

The simulation results demonstrate that, for optimal performance, a plug-in hybrid electric vehicle should alternate between the combustion engine and the electric motor. Moreover, the simulation reveals that in none of the scenarios examined is it advisable to rely solely on the electric motor for the entire daily commute, even if the battery can supply sufficient energy for the trip. In fact, across all simulated cases with varying driving modes and speed ranges, the time fraction during which the electric motor alone powers the PHEV never reaches 100%. This outcome confirms the necessity of a shared power source. Regarding the shared power source, simulation results indicate that the daily fractional use of the electric motor increases as the vehicle speed range decreases. This trend is observed regardless of the driving mode or combustion engine type (Figure 1).

Similarly, we analyze the evolution of the f_{EM} coefficient across vehicle segments as a function of vehicle speed for each driving mode. The coefficient is very similar for the high and intermediate segments, showing a difference of less than 1%. For the low segment, the decrease is 8%, on average (Figure 2)

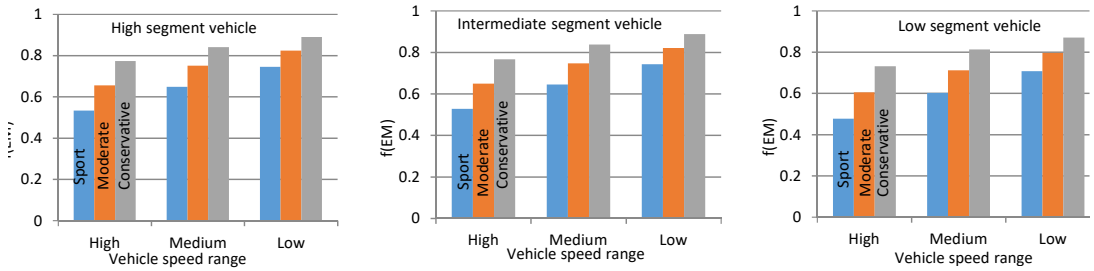

Figure 1: Evolution of Electric Motor Fractional time with Driving Mode and Vehicle Speed Range for the Gasoline PHEV for Different Vehicle Segments

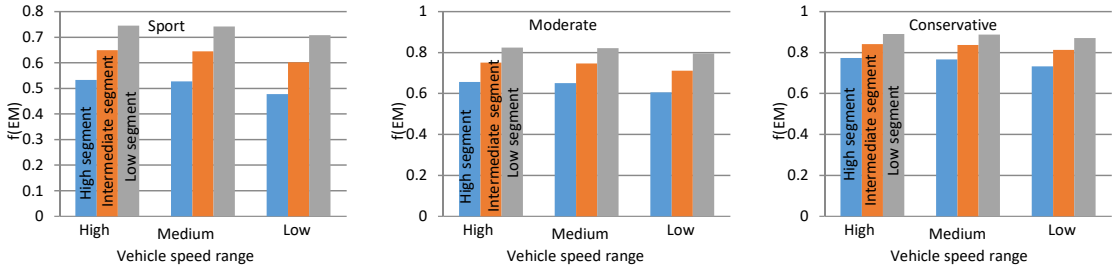

Figure 2: Evolution of Electric Motor Fractional Time for the Different Vehicle Segments as a Function of the Vehicle Speed Range for Every Driving Mode

As a result, daily electrical energy consumption also rises with a reduction in the vehicle speed range. Repeating the graph representation of the fEM coefficient in Figure 1, we obtain (Figure 3):

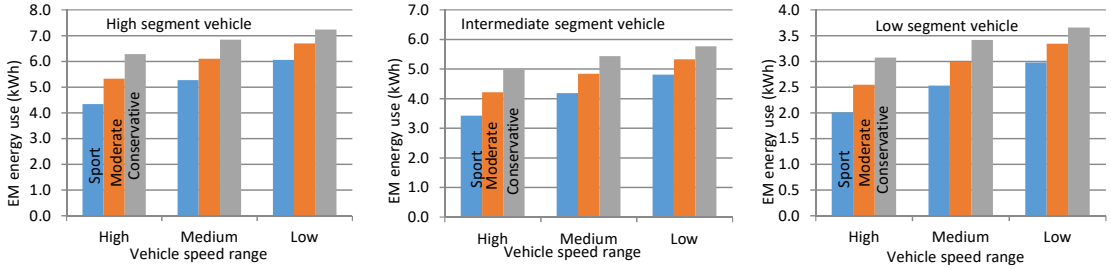

Figure 3: Evolution of Electric Energy use with Driving Mode and Vehicle Speed Range for the Gasoline PHEV for Different Vehicle Segments

However, the driving range achievable with the electric motor alone decreases due to higher energy usage (Figure 4). Conversely, the percentage gain in total driving range from electric operation diminishes as the vehicle speed range narrows across all driving modes and engine types.

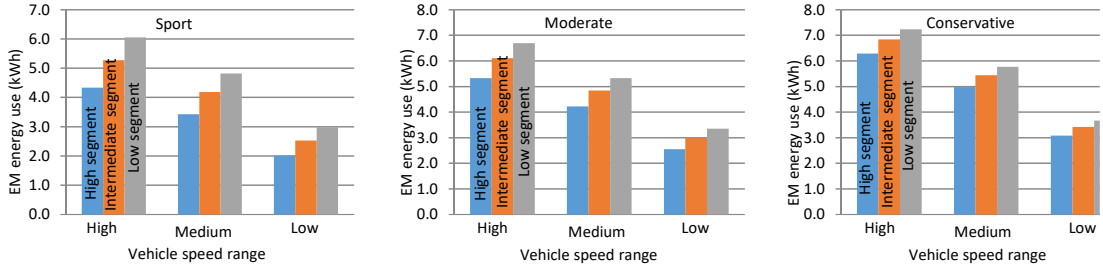

Figure 4: Evolution of Electric Energy use for the Different Vehicle Segments as a Function of the Vehicle Speed Range for Every Driving Mode

A significant reduction in electric energy consumption is observed as the vehicle speed range decreases, with the effect being most pronounced at the lowest speed range. Consequently, operating the vehicle at lower speed ranges proves to be the most effective strategy for minimizing energy use in electric mode. On average, transitioning from a high to an intermediate speed range results in a 26% reduction in electric energy use, while switching from a high to a low speed range yields a reduction of 109.4%.

Optimizing electric energy consumption extends the driving range, measured by the number of days the vehicle can operate solely on electric power. As shown in Table 7, the electric-mode driving range varies according to vehicle segment and combustion engine type.

Comparing the different vehicle categories' values, we observe similar driving range in electric mode, 2.6 and 4.3 days for the high segment, 2.5 to 4.2 days for the intermediate segment, and 2.4 and 4.4 days for the low segment. These values correspond to the gasoline PHEV; if we operate with the diesel PHEV, the driving ranges are 2.5 and 3.5 days for the high category, 2.4 and 3.3 days for the intermediate, and 2.3 and 3.4 days for the low. The lower driving range reason, if operating in electric mode with the diesel PHEV, is the higher combustion engine efficiency. The higher efficiency results in a lower ratio of electric to combustion engine time during the daily commute.

7.Control System

Battery management optimization requires a control process to regulate the operational time of the combustion engine and electric motor during the daily commute. The control process should evaluate the optimal conditions for engaging or disengaging the electric motor, with this power source as the default option for vehicle propulsion.

Since we have demonstrated from the simulation process that running on the electric motor the entire daily journey is not optimum, the control system regulates the electric motor's daily working time according to values derived from the simulation for the vehicle type and category and driving conditions, it is said, driving mode, and vehicle speed range.

A daily journey in urban areas involves changes in driving conditions and power requirements; therefore, the control system should engage and disengage the electric motor at a specific power threshold to meet the optimum performance conditions defined by the coefficient f_{EM}. Nevertheless, it is difficult to predict the electric motor engagement time for a daily commute without precise knowledge of the journey's path and traffic conditions; for this reason, the control system requires previous information about these parameters and the driving mode.

To achieve this objective, the control process begins by prompting the driver to choose a driving mode for the daily commute, sport, moderate, or conservative. Following this, the control system requests the driver to enter the destination into the vehicle's navigation system and select a preferred route from various available options. After the driver chooses the roadway, the control system assesses traffic conditions for each roadway segment and calculates the permissible speed for the entire journey.

Using the provided information about driving mode and vehicle speed range, the control system retrieves the f_{EM} coefficient from the database, calculates the electric energy use for the corresponding path segment, and the operating time, t_{EM}, representing the time for the electric motor operation. The control system, then, engages the electric motor for a time equal to t_{EM}, after which it disengages the electric motor and switches to the combustion engine.

The control system operates automatically, continuously checking the vehicle's speed range and driving mode; therefore, if either of these conditions changes, the control system changes the f_{EM} value and recalculates the electric motor operating time, t_{EM}. Figure 5 shows the control system operational flowchart.

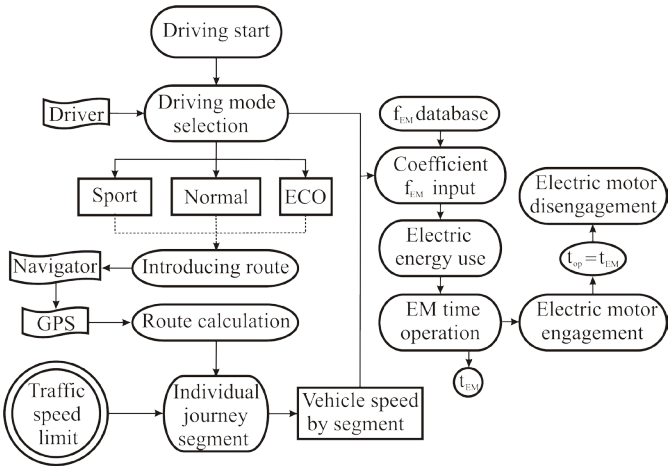

Figure 5: Control System Operational Flowchart

The control system engages the electric motor based on the power demand for specific driving conditions. Knowing the information about the route, the control system determines the energy consumption for every route segment using Equation 3, retrieving the corresponding f_{EM} value for the specific segment from the database to determine the electric energy use, and the average electric power demand through the classical expression:

$$P_i = \frac{\xi_{EM,i}}{t_{dr,i}} = f_{EM,i}\frac{\xi_i}{t_{dr,i}} = f_{EM,i}\left[ma_i v_i + \kappa v_i^2 + mg(\mu + \sin\alpha_i)v_i\right] \quad (22)$$

The P_i value represents the power threshold that the control system uses to regulate the electric motor. If the power demand is above the threshold, the control system disengages the electric motor; otherwise, the electric motor remains engaged.

8. Experimental Tests Conditions

Experimental tests run on rented vehicles of the selected PHEV models. Due to the difficulties in running the vehicles for long time, the experimental tests for every car model reduce to nine days. We carried out tests in urban area, downtown and peripheral, to reproduce simulated driving conditions in the most accurate way. We developed experimental tests on plug-in hybrid electric vehicles with a gasoline combustion engine, since there are no commercial models with a diesel engine. Since the rented commercial vehicles do not include a control system like the one proposed in this work, it was necessary to resort to a manual control system, which connected and disconnected the electric motor manually by activating the electric motor connection/disconnection button at the time established by the theoretical simulation. To this goal, we hired the service of a co-pilot who controlled said time and the connection/disconnection system.

To facilitate the co-pilot's task and better adjust to driving conditions, we previously drove the route used for the experimental tests at various times of day to obtain accurate information on the current speed limit for each path section. Since the speed range can vary with the time of day, we decided to average the results when data dispersion was low, which is indeed the situation. We transferred all the information gathered in the previous tests to a table that the co-pilot used as a reference database for the manual control of electric motor engagement and disengagement. We conducted three consecutive tests for each driving mode and vehicle model. Each test lasted one day, combining urban and suburban routes, with a daily distance covered of 157.55 km for the Volvo XC90 and Toyota Prius, and 148.7 km for the Ford Kuga, which equates to a range of two days according to the WLTP cycle for each used vehicle.

The daily test included a morning and an afternoon session with a charge process between them. We used a fast-charging station to recharge the battery during the time lapse between tests. The average recharge time depends on the vehicle model, the manufacturer's maximum charging specs, and battery capacity. Table 8 lists the charging time for the selected models at full battery charge.

Vehicle model	Battery capacity (kWh)	Max. Charging (kW)	Charge time (h)
Volvo XC90	18.8	6.4	2.94
Ford Kuga	14.4	3.7	3.89
Toyota Prius	8.8	3.7	2.38

Table 8: Charging Specifications for the Selected Models

The test average speed depends on traffic conditions; however, the variations are of low significance since we ran tests at the same hour interval in the morning and in the afternoon. The nine test days for every car model correspond to a combination of every one of the following cases (Table 9):

Driving mode	Path type	Average speed (km/h)
Sport	Peripheral	66.8
	Peripheral/Downtown	64.0
	Downtown	59.0
Moderate	Peripheral	57.3
	Peripheral/Downtown	56.0
	Downtown	54.0
Conservative	Peripheral	48.5
	Peripheral/Downtown	47.8
	Downtown	46.3

Table 9: Test Run Characteristics

The average speed for each vehicle is calculated by dividing the distance traveled by the travel time. Travel time ranges from 1.18 hours to 1.7 hours per session. Therefore, the maximum overall time for the daily test is 5.6 hours for the Ford Kuga, driving in conservative mode on an urban road. The minimum of 3.6 h corresponds to the Toyota Prius, driving sportily on a ring road. Since the daily overall time is excessive for a single driver, the pilot and co-pilot exchange duties from morning to afternoon.

Urban driving conditions today are characterized by variable vehicle speeds, making it challenging to maintain a consistent vehicle speed range for daily commutes. Therefore, we have to determine the effective correction factor for the electric motor driving range, EM-DR ratio in Table 6, which matches current driving conditions. Since the EM-DR ratio depends on the driving mode and vehicle speed range, provided we run for a given driving mode, we determine the ratio value by applying the following expression:

$$(EM-DR)_{eff} = \sum_{i=1}^{3} (EM-DR)_i (f_{vs})_i \quad (23)$$

(*EM-DR*) is the coefficient corresponding to every vehicle speed range, high, medium, and low, and fvs represents the time fraction over the daily journey corresponding to the selected vehicle speed range. Subscripts i=1, 2, and 3 correspond to high, medium, and low vehicle speed range.

Applying Equation 22 to values in Table 6, we have (Table 10):

Path type →	Peripheral	Peripheral/Downtown	Downtown
Volvo XC90	1.690	1.603	1.457
	1.418	1.368	1.282
	1.236	1.208	1.160
Ford Kuga	1.705	1.615	1.465
	1.428	1.376	1.288
	1.244	1.215	1.165
Toyota Prius	1.855	1.744	1.557
	1.515	1.451	1.342
	1.292	1.256	1.196

Table 10: Corrected Values of the EM-DR Ratio for the Current Driving Conditions in the Experimental Tests

The setup driving conditions for the vehicle speed range concerns correspond to the following schedule (Table 11):

	Vehicle speed range		
Path type	High	Medium	Low
Peripheral	0.5	0.4	0.1
Peripheral/Downtown	0.3	0.5	0.2
Downtown	0.1	0.3	0.6

Table 11: Fraction over the Daily Journey Time

The data shown in Table 11 correspond to the average values over the experimental test measurements.

9. Experimental Tests Results

The experimental results correspond to a complete battery discharge test, giving the driving range of the PHEV operating in electric mode. Figure 6 displays the values of every case according to test run characteristics shown in Table 9.

The X-axis labels account for the following driving conditions:

- Sport driving mode and peripheral pathway (Sp-Periph.)
- Sport driving mode and peripheral and downtown combined pathway (Sp-Per-Down)
- Sport driving mode and downtown pathway (Sp-Down)
- Moderate driving mode and peripheral pathway (Mod-Periph.)
- Moderate driving mode and peripheral and downtown combined pathway (Mod-Per-Down)
- Moderate driving mode and downtown pathway (Mod-Down)
- Conservative driving mode and peripheral path way (Con-Periph.)
- Conservative driving mode and peripheral and downtown combined path way (Con-Per-Down)
- Conservative driving mode and downtown path way (Con-Down)

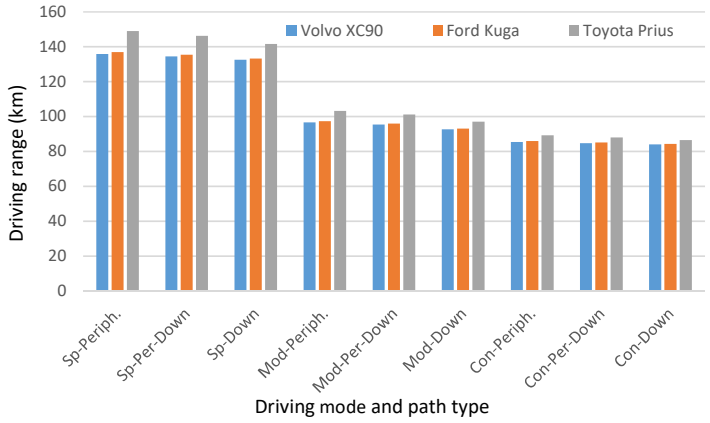

Figure 6: Driving Range as a Function of the Driving Mode and Path type

We observed that the experimental results show a greater range than that provided by the manufacturer according to the WLTP protocol. This increase is due to the shorter electric motor operating time, which reduces energy consumption and, consequently, extends battery life.

This situation is perfectly compatible with PHEV operation with a dual power supply, as the study analyzes the optimal performance of electrical energy use supplied by the battery in combination with the combustion engine.

Regarding performance improvement, the EM-DR ratio provides a clear indication of how optimal electric motor management benefits the PHEV's daily journey development. This coefficient serves as a behavior enhancement index for the energy supply system, linking it to global energy consumption and efforts to minimize greenhouse gas emissions.

We show in Figure 7 the performance gain factor as a function of the driving mode and path type.

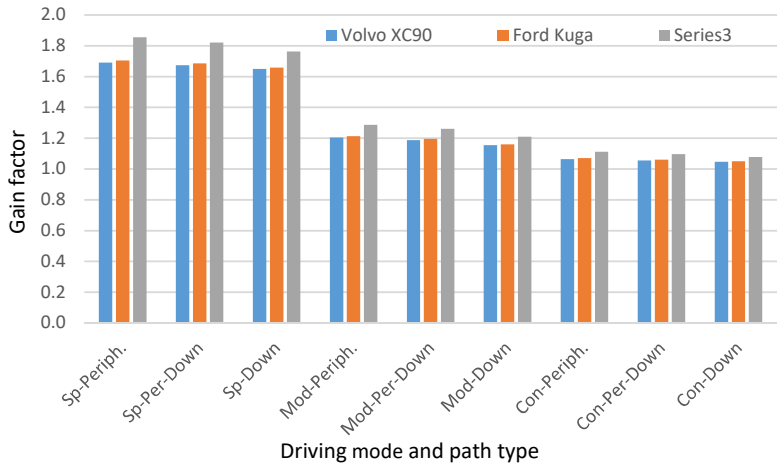

Figure 7: Performance Gain Factor as a Function of the Driving Mode and Path Type

It appears that energy management performance enhances when driving aggressively (sport mode) due to the higher power demands associated with that style of driving. This situation creates a broader scope for performance improvement. Additionally, both moderate and conservative driving modes exhibit similar performance results, though the moderate mode tends to show a slightly greater improvement.

The data presented in Figure 7 shows that sport driving mode yields an average performance improvement of 1.722, followed by moderate at 1.207, and conservative at 1.069. This situation indicates that while conservative driving (ECO mode) is very efficient, it only achieves a performance improvement of around 7% when the control system manages the electric motor.

On the other hand, it is necessary to compare the gain factor obtained in the experimental results with the predicted values by the simulation to verify the validity of the simulation process. Doing so, we have (Figure 8):

We are aware that experimental data and simulation predictions differ for almost any driving mode and track type. This difference is due to manual management of the electric mode control, which introduces a delay in the electrical response, producing a discrepancy between experimental data and simulation results. However, this discrepancy is insignificant, less than 1.4% in all cases. Figure 9 shows the deviation in simulation prediction regarding experimental values.

Considering all the tests, the overall average deviation between the experimental data and the simulation prediction is 0.1%, which is negligible for predicting performance improvements. Therefore, we can validate the simulation for improved PHEV performance prediction when the electric motor control system is implemented.

While the experimental tests apply to gasoline-powered PHEVs, the strong correlation between the experiments and the simulation allows us to extend the validity of the proposed procedure to diesel-powered PHEVs.

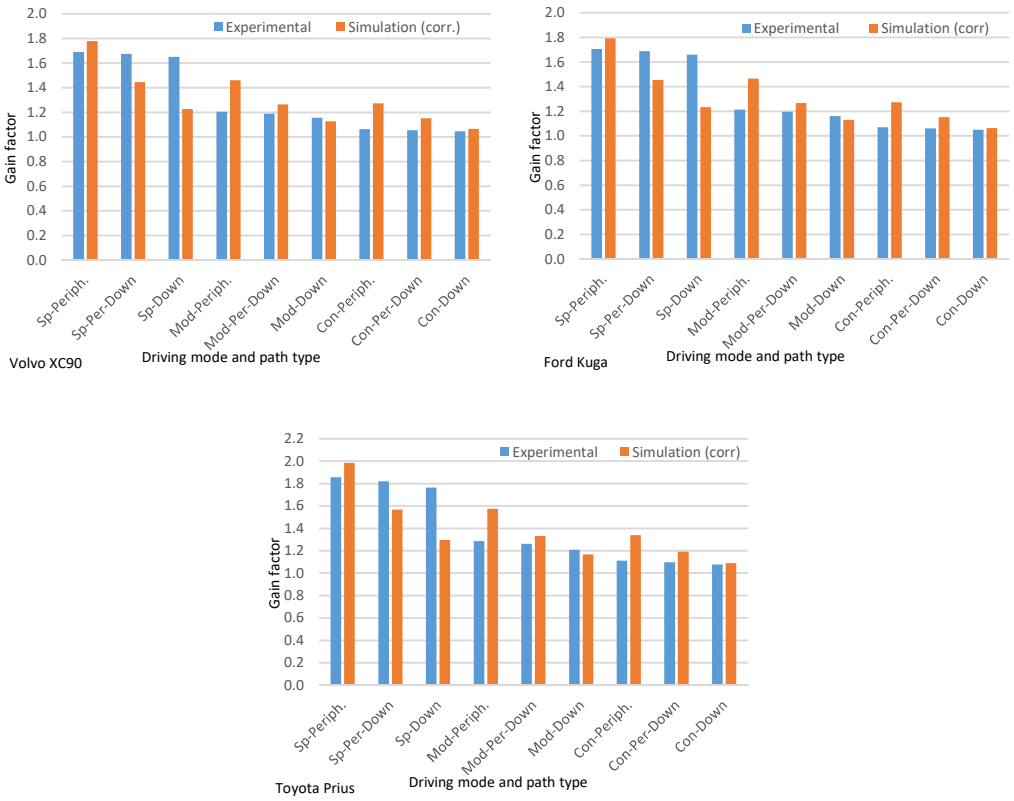

Figure 8: Comparative Analysis of Experimental and Simulation Data for the Performance Improvement Coefficient

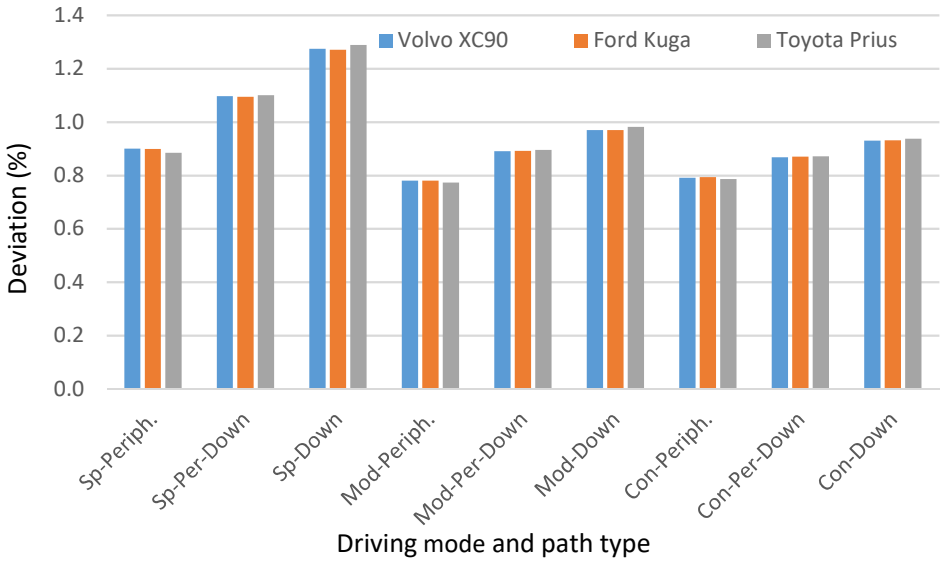

Figure 9: Deviation between Experimental data and Simulation Prediction of the Performance Improvement for Variable Driving Modes and Path types in PHEVs

10. Conclusions

Implementing a control system to regulate the electric motor in plug-in hybrid vehicles improves vehicle performance and optimizes energy consumption. Performance improvements reach up to 72.2% in Sport mode, where aggressive driving demands greater power. Precise management of the electric motor by the control system, with programmed coupling and decoupling, not only benefits the performance of the PHEV but also reduces energy consumption and greenhouse gas emissions. Furthermore, the control system extends the PHEV's range in electric mode by improving electric power supply management, activating and deactivating the electric motor at the appropriate time during the daily commute.

The simulation used to predict improvements in energy management was validated through experimental testing with 98.6% accuracy, even under the worst driving conditions. Analysis of the simulation of a complete daily commute matched experimental driving with 99.9% accuracy, demonstrating the high predictive power of the daily commute. While the experimental tests apply to gasoline-powered PHEVs, the strong correlation between the experiments and the simulation allows us to extend the validity of the proposed procedure to diesel-powered PHEVs.

References

1. Bryhadyr, I., Panova, I., & Strelianyi, V. (2021). Transition from internal combustion engines to electric motors–legal and organizational dimensions. *Studia nad Bezpieczeństwem*, (6), 77-85.
2. de Almeida, A. T., Ferreira, F. J., & Fong, J. (2023). Perspectives on electric motor market transformation for a net zero carbon economy. *Energies, 16*(3), 1248.
3. King, M. F. L., Baruch, J., & Elayarani, E. (2024). Transitions from IC engine to EV and HEV. In *Energy Efficient Vehicles* (pp. 96-125). CRC Press.
4. Todorovic, M., & Simic, M. (2018, June). Current state of the transition to electrical vehicles. In *International Conference on Intelligent Interactive Multimedia Systems and Services* (pp. 130-139). Cham: Springer International Publishing.
5. Greene, D. L., Park, S., & Liu, C. (2014). Analyzing the transition to electric drive vehicles in the US. *Futures, 58*, 34-52.
6. Altenburg, T. (2014). *From combustion engines to electric vehicles: a study of technological path creation and disruption in Germany* (No. 29/2014). Discussion Paper.
7. Gruden, D. (2019). Will Electric Motor Substitute Internal Combustion Engine?. *Mobil. Veh. Mech, 45*(4), 19-31.
8. Ağbulut, Ü., & Bakır, H. (2019). The investigation on economic and ecological impacts of tendency to electric vehicles instead of internal combustion engines. *Düzce Üniversitesi Bilim ve Teknoloji Dergisi, 7*(1), 25-36.
9. Todorovic, M., Simic, M., & Kumar, A. (2017). Managing transition to electrical and autonomous vehicles. *Procedia computer science, 112*, 2335-2344.
10. [10] Bauer, G. (2018). The impact of battery electric vehicles on vehicle purchase and driving behavior in Norway. *Transportation Research Part D: Transport and Environment, 58,* 239-258.
11. Tu, J. C., & Yang, C. (2019). Key factors influencing consumers' purchase of electric vehicles. *Sustainability, 11*(14), 3863.
12. Bessenbach, N., & Wallrapp, S. (2013). Why do consumers resist buying electric vehicles. *An empirical study of innovation perception and the effect of consumer characteristics, innovation exposure and buying incentives.*
13. Rudolph, C. (2016). How may incentives for electric cars affect purchase decisions?. *Transport Policy, 52,* 113-120.
14. Mandys, F. (2021). Electric vehicles and consumer choices. *Renewable and Sustainable Energy Reviews, 142*, 110874.
15. Liu, Y., Zhao, X., Lu, D., & Li, X. (2023). Impact of policy incentives on the adoption of electric vehicle in China. *Transportation research part A: policy and practice, 176*, 103801.
16. Li, Y., Liang, C., Ye, F., & Zhao, X. (2023). Designing government subsidy schemes to promote the electric vehicle industry: A system dynamics model perspective. *Transportation Research Part A: Policy and Practice, 167*, 103558.
17. Liu, X., Sun, X., Zheng, H., & Huang, D. (2021). Do policy incentives drive electric vehicle adoption? Evidence from China. *Transportation Research Part A: Policy and Practice, 150,* 49-62.
18. Ajeigbe, K., & Holt, W. (2025). Government Policies and Incentives for EV Manufacturing.
19. Langbroek, J. H., Franklin, J. P., & Susilo, Y. O. (2016). The effect of policy incentives on electric vehicle adoption. *Energy Policy, 94*, 94-103.
20. Wee, S., Coffman, M., & La Croix, S. (2018). Do electric vehicle incentives matter? Evidence from the 50 US states. *Research Policy, 47*(9), 1601-1610.
21. Diamond, D. (2009). The impact of government incentives for hybrid-electric vehicles: Evidence from US states. *Energy policy, 37*(3), 972-983.
22. Sierzchula, W., Bakker, S., Maat, K., & Van Wee, B. (2014). The influence of financial incentives and other socio-economic factors on electric vehicle adoption. *Energy policy, 68,* 183-194.
23. Trends in electric car markets. Global EV Outlook 2025.
24. The global electric vehicle market overview in 2025. VIRTA.
25. Electric vehicles worldwide – statistics & facts. Statista.
26. Electric car use by country. Wikipedia.
27. Deng, J., Bae, C., Denlinger, A., & Miller, T. (2020). Electric vehicles batteries: requirements and challenges. *Joule, 4*(3), 511-515.
28. Sanguesa, J. A., Torres-Sanz, V., Garrido, P., Martinez, F. J., & Marquez-Barja, J. M. (2021). A review on electric vehicles: Technologies and challenges. *Smart Cities, 4*(1), 372-404.
29. Suciu, G., & Pasat, A. (2017, March). Challenges and opportunities for batteries of electric vehicles. In *2017 10th international symposium on advanced topics in electrical*

engineering (ATEE) (pp. 113-117). IEEE.
30. S. Rangarajan, S., Sunddararaj, S. P., Sudhakar, A. V. V., Shiva, C. K., Subramaniam, U., Collins, E. R., & Senjyu, T. (2022). Lithium-ion batteries—The crux of electric vehicles with opportunities and challenges. *Clean Technologies, 4*(4), 908-930.
31. Alanazi, F. (2023). Electric vehicles: benefits, challenges, and potential solutions for widespread adaptation. *Applied sciences, 13*(10), 6016.
32. Chan, C. C., & Chau, K. T. (1996, August). An overview of electric vehicles-challenges and opportunities. In *Proceedings of the 1996 IEEE IECON. 22nd International Conference on Industrial Electronics, Control, and Instrumentation* (Vol. 1, pp. 1-6). IEEE.
33. Krishna, G. (2021). Understanding and identifying barriers to electric vehicle adoption through thematic analysis. *Transportation Research Interdisciplinary Perspectives, 10*, 100364.
34. Curtin, R., Shrago, Y., & Mikkelsen, J. (2009). Plug-in hybrid electric vehicles. *Reuters/University of Michigan, Surveys of Consumers*, 318-9.
35. Komatsu, M., Takaoka, T., Ishikawa, T., Gotouda, Y., Suzuki, N., & Ozawa, T. (2008). *Study on the potential benefits of plug-in hybrid systems. SAE International.*
36. Plug-in hybrids pollute almost as much as petrol cars, report finds – EU Data. Transport & Environment. 16 October 2025.
37. Smoke screen: the growing PHEV emissions scandal. Transport & Environment.
38. Plötz, Patrick, Gnann, Till. Analysis: Real-world Fuel Consumption and Potential Future Regulation of Plug-In Hybrid Electric Vehicles in Europe – An Empirical Analysis of about one Million Vehicles. Ariadne Kopernikus Projekte.
39. Tulpule, P., Marano, V., & Rizzoni, G. (2009, June). Effects of different PHEV control strategies on vehicle performance. In *2009 American control conference* (pp. 3950-3955). IEEE.
40. Gong, Q., Tulpule, P., Marano, V., Midlam-Mohler, S., & Rizzoni, G. (2011, June). The role of ITS in PHEV performance improvement. In *Proceedings of the 2011 American control conference* (pp. 2119-2124). IEEE.
41. Wirasingha, S. G., & Emadi, A. (2010). Classification and review of control strategies for plug-in hybrid electric vehicles. *IEEE Transactions on vehicular technology, 60*(1), 111-122.
42. Sharer, P. B., Rousseau, A., Karbowski, D., & Pagerit, S. (2008). *Plug-in hybrid electric vehicle control strategy: Comparison between EV and charge-depleting options* (No. 2008-01-0460). SAE Technical Paper.
43. Karbowski, D., Rousseau, A., Pagerit, S., & Sharer, P. (2006, October). Plug-in vehicle control strategy: from global optimization to real time application. In *Proceedings of 22th International Electric Vehicle Symposium* (pp. 1-12).
44. Rosu, Ioanid. (2002) The Bellman principle of optimality.
45. Marano, V., Tulpule, P., Stockar, S., Onori, S., & Rizzoni, G. (2009). Comparative study of different control strategies for plug-in hybrid electric vehicles (No. 2009-24-0071). SAE Technical Paper.
46. Recalde, A., Cajo, R., Velasquez, W., & Alvarez-Alvarado, M. S. (2024). Machine learning and optimization in energy management systems for plug-in hybrid electric vehicles: a comprehensive review. *Energies, 17*(13), 3059.